Polychromatic vectorial vortex formed by geometric phase elements

Avi Niv, Gabriel Biener, Vladimir Kleiner, and Erez Hasman

Optical Engineering Laboratory, Faculty of Mechanical Engineering, Technion–Israel Institute of Technology, Haifa 32000, Israel

Received November 16, 2006; accepted January 2, 2007;
posted January 16, 2007 (Doc. ID 77166); published March 5, 2007

We propose the use of a geometric phase, obtained by spatial polarization state manipulations, for the formation of polychromatic vectorial vortices. Experimental demonstration is obtained by using Pancharatnam–Berry phase optical elements formed by a space-variant subwavelength grating etched on a GaAs wafer. We further demonstrate formation of scalar and unpolarized polychromatic vortices. © 2007 Optical Society of America

OCIS codes: 050.2770, 260.5430.

In the past few years, researchers have directed increased attention to phase singularities in polychromatic beams,[1] and to polychromatic vortices, in particular.[2] It is expected that polychromatic vortices will enable formation of femtosecond laser pulses with angular momentum[3] and advanced applications such as stellar coronagraphy.[4,5] Consequently, several methods for embedding vortices in polychromatic fields have been devised. Such methods include using a uniaxial crystal,[6] a dispersion compensated hologram,[3,7,8] and spiral phase elements composed of two materials with opposite dispersion.[9]

In addition to the scalar singular optics, research in vectorial singular optics, including vectorial vortices, has been conducted.[10–13] However, none of these studies considered embedding vectorial vortices in a polychromatic beam. A vectorial vortex occurs around a point where a scalar vortex is centered in at least one of the scalar components of the vectorial wave fields. It is expected that polychromatic vectorial vortices will be useful in applications such as hollow fiber polychromatic power delivery[13] and surface wave excitation by radially polarized pulses or polychromatic beams.[14]

In this Letter we experimentally demonstrate the formation of linearly polarized vectorial vortices embedded in a polychromatic beam based on a geometric phase that accompanies space-variant polarization state manipulation. We form our vectorial vortices by using space-variant subwavelength gratings. These elements, which apply geometric phase modulation, are termed Pancharatnam–Berry phase optical elements[15,16] (PBOEs). In addition, we experimentally demonstrate formation of unpolarized vortices. These beams are the incoherent sum of two polychromatic scalar vortices at orthogonal circular polarizations. The formation of a polychromatic scalar vortex is also discussed.

A subwavelength grating behaves as a uniaxial crystal with the optical axis parallel and perpendicular to the grating stripes.[15] PBOEs are obtained by spatially rotating the orientation of the subwavelength grating's grooves along the face of an element. In this manner, PBOEs operate as space-variant retarders or polarizers. The Jones matrix of a PBOE can be found by applying the two-dimensional rotation matrix to a Jones matrix of a uniform retarder, resulting in[15]

$$\mathbf{T}(x,y;\lambda) = \eta_0(\lambda)\mathbf{I} + \eta_1(\lambda)\{|R\rangle\langle L|\exp[i2\theta(x,y)] + |L\rangle\langle R|\exp[-i2\theta(x,y)]\}, \quad (1)$$

where $\mathbf{I}$ is the 2×2 identity matrix, $\theta(x,y)$ is the local subwavelength groove orientation, x and y form the rectangular axes, λ is the wavelength, and $|R\rangle$, $|L\rangle$ are the right- and left-handed circularly polarized unit vectors in the Dirac bracket notation. Also, $\eta_0(\lambda)=\{t_x(\lambda)+t_y(\lambda)\exp[i\phi(\lambda)]\}/2$ and $\eta_1(\lambda)=\{t_x(\lambda)-t_y(\lambda)\exp[i\phi(\lambda)]\}/2$, where $\phi(\lambda)$ is the subwavelength grating's retardation and $t_x(\lambda)$, $t_y(\lambda)$ are the amplitude transmissions parallel and perpendicular to the subwavelength grooves. For dielectric subwavelength gratings, the transmission is relatively high; thus $t_x \cong t_y \cong 1$ and the retardation is given by $\phi(\lambda)=\phi_0\lambda_0/\lambda$, where $\phi_0=\phi(\lambda_0)$ for the central wavelength λ_0.

According to Eq. (1), the beam that emerges from a PBOE with $\phi_0=\pi$ and $\theta=m\varphi/2$ (φ is the azimuth in polar coordinates, m is an integer), and that is illuminated by a polychromatic beam, $|E_{\text{in}}\rangle=\sqrt{S(\lambda)}|L\rangle$ [$S(\lambda)$ is the spectrum], is

$$|E_{\text{out}}(\lambda)\rangle = \mathbf{T}|E_{\text{in}}\rangle = \sqrt{S(\lambda)}[\eta_0(\lambda)|L\rangle + \eta_1(\lambda)\exp(im\varphi)|R\rangle]. \quad (2)$$

Equation (2) represents a vectorial vortex beam composed of two coherent polarization components. The first maintains the polarization of the incident beam and bears no phase modification; the second is orthogonally polarized and has the phase of a scalar vortex. The magnitudes of the two polarization components are governed by $\eta_0(\lambda)$ and $\eta_1(\lambda)$. At the design wavelength, $\eta_0=0$. Thus a pure scalar vortex is formed. However, for other spectral components this is not the case, and Eq. (2) cannot be considered a polychromatic scalar vortex. However, if the left-handed circular polarized component is removed from the beam, we obtain

0146-9592/07/070847-3/$15.00

$$|E\rangle = \sqrt{S(\lambda)}\,\eta_1(\lambda)\exp(im\varphi)|R\rangle. \quad (3)$$

Consequently, a polychromatic scalar vortex with a topological charge m is achieved. Removal of the undesired component can be obtained either by using a suitable achromatic circular polarizer or by spatial filtering. The spatial filtering is simple, as the undesired component has a zero spatial frequency and thus can be easily filtered by a 4-f system. The dispersion manifests itself through $\eta_1(\lambda)$, which modifies the spectrum of the emerging beam while leaving the phase intact. It is important to note that careful design of the subwavelength groove profile can yield a birefringence that is proportional to the wavelength, at least within a limited spectral band.[17,18] Thus an achromatic subwavelength grating retarder is formed, which can serve to retain the power spectrum.

An important feature of Eq. (3) is the added phase factor, $m\varphi$. This phase originates solely from the local changes in the polarization state of the emerging beam. It is easy to show this dependence by using the Poincaré sphere presentation (see Fig. 1). In the described example, mapping of the polarization state of the emerging beam at two distinct points on the element shows them to travel along different geodesic lines. Polarization state changes at these two locations are represented by the geodesic lines connecting the north and the south poles of the sphere. Half of the area enclosed by these geodesic lines, i.e., $\Omega/2$, is $2\theta = m\varphi$, which is exactly the phase modification as described in Eq. (3). As can be seen, the phase modification depends only on the space-variant retarder orientation and is therefore independent of the wavelength.

From Eq. (1), illuminating the PBOE discussed above with a linearly polarized polychromatic beam, $|E_{\text{in}}\rangle = \sqrt{S(\lambda)}|H\rangle$ [where $|H\rangle = (|R\rangle + |L\rangle)/2$], results in

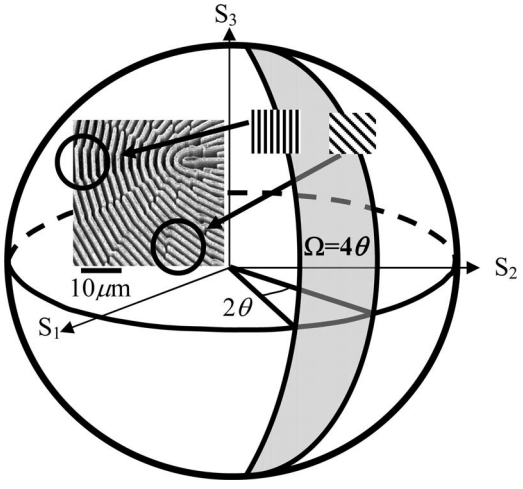

Fig. 1. Polarization state transformation is represented as trajectories on the Poincare sphere. Rotation of the grating by θ results in a 2θ phase modification. This phase equals half of the area enclosed by the geodesic lines. Inset, scanning electron microscope image of the PBOE surface for $m = 1$.

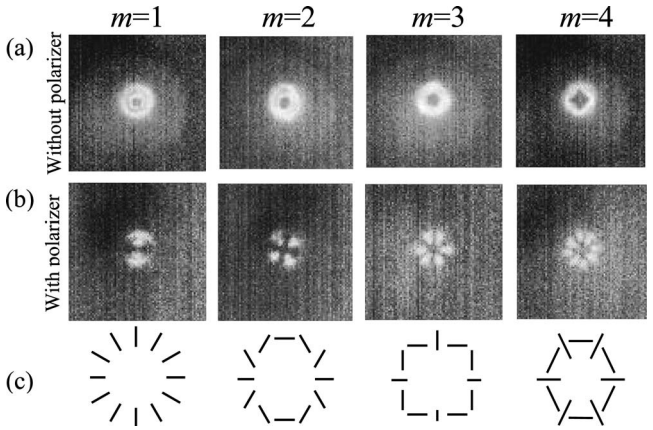

Fig. 2. (a) Measured intensity distributions for linearly polarized vectorial vortices embedded in polychromatic beams. (b) Same as (a) but imaged through a linear analyzer. (c) Schematic representation of the polarization state of the linearly polarized vectorial vortices.

$$|E_{\text{out}}(\lambda)\rangle = \mathbf{T}|E_{\text{in}}\rangle = \eta_0(\lambda)|H\rangle + \eta_1(\lambda)|\varphi_m\rangle, \quad (4)$$

where $|\varphi_m\rangle = |R\rangle\exp(im\varphi) + |L\rangle\exp(-im\varphi)$ denotes a linearly polarized vectorial vortex with a polarization order number m.[10] The emerging beam is composed of a horizontally polarized component of magnitude $\eta_0(\lambda)$ and a linearly polarized vectorial vortex of magnitude $\eta_1(\lambda)$. At the design wavelength, $\eta_0 = 0$, a pure linearly polarized axially symmetric vectorial vortex is formed. However, for other spectral components, this beam is not a vectorial vortex. Nevertheless, the undesired $|H\rangle$ component can be spatially filtered so as to form a linearly polarized vectorial vortex. As described in the former case, the spatial filtering is simple, as it again involves zero spatial frequency of the undesired component.

To experimentally demonstrate our approach, we used PBOEs, originally designed to introduce a helical phase for circular illumination at a nominal wavelength of 10.6 μm. A scanning electron microscope image of this PBOE is shown in the inset of Fig. 1. The elements are 10 mm in diameter and composed of a 2 μm subwavelength period etched 5 μm onto a GaAs wafer with a fill factor of 0.5. A more thorough description of the design and fabrication of the PBOEs can be found in Ref. 16. The PBOE was illuminated with a beam from a collimated SiC thermal source transmitted through an achromatic wire grid polarizer. Images were captured by using a bolometric camera (FLIR Thermovision A40). Figure 2(a) shows the far-field intensity distribution of the linearly polarized vectorial vortex for the various polarization order numbers. Note that the intensity images are integrated over the responsivity band of the camera, which is between 8 and 14 μm in wavelength. We calculated $\eta_0(\lambda)$ and $\eta_1(\lambda)$ for our measured groove profile by using rigorous coupled wave analysis. The average value of $|\eta_0(\lambda)|^2/|\eta_1(\lambda)|^2$ was found to be less than 5% within this spectral band. Thus the central intensity lobe is small and vanishes within the background radiation. Figure 2(b) shows the imaged intensity distribution transmitted

through a polarizer analyzer. The propellerlike intensity shape confirms the existence of a polychromatic linearly polarized vectorial vortex, shown schematically in Fig. 2(c).

Another interesting case is the unpolarized illumination of our PBOE. Figures 3(a) and 3(b) show the measured far-field intensities when the two polarizers are removed. The emerging beam is the incoherent sum of two polychromatic scalar vortices at orthogonal circular polarizations. Unpolarized vortices are sufficient for applications that require neither polarized light nor the transfer of an angular momentum. For comparison, we included Fig. 3(c), which shows the experimental far-field intensity distribution from a ZnSe refractive helical phase device with a topological charge of unity that is designed for a nominal 10.6 μm wavelength. The apparent dark fringe that splits the intensity doughnut results from phase discontinuity, as predicted by Berry.[19]

To conclude, we propose the use of a geometric phase induced by space-variant polarization state manipulation to form polychromatic vectorial, unpolarized, and scalar vortices. Polychromatic linearly polarized vectorial vortices and polychromatic unpolarized vortices were experimentally demonstrated, using PBOEs realized by space-variant subwavelength gratings.

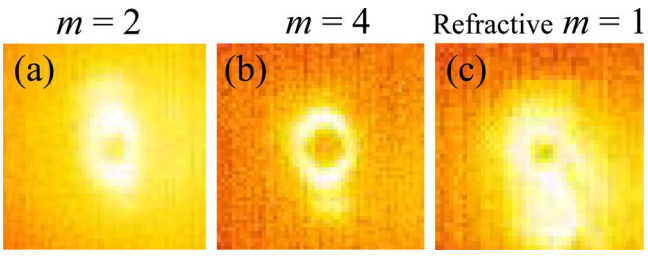

Fig. 3. (Color online) Measured intensity distributions for unpolarized vortices with $m=2,4$ in (a) and (b), respectively. (c) Measured diffraction pattern obtained from a refractive spiral phase plate for $m=1$.

E. Hasman's e-mail address is mehasman@tx.technion.ac.il.

References

1. G. Gbur, T. D. Visser, and E. Wolf, Phys. Rev. Lett. **88**, 013901 (2002).
2. M. V. Berry, New J. Phys. **4**, 66 (2002).
3. K. Bezuhanov, A. Dreischuh, G. G. Paulus, M. G. Schätzel, and H. Walther, Opt. Lett. **29**, 1942 (2004).
4. D. Mawet, P. Riaud, O. Absil, and J. Surdej, Astrophys. J. **633**, 1191 (2005).
5. G. Foo, D. M. Palacios, and G. A. Swartzlander, Jr., Opt. Lett. **30**, 3308 (2005).
6. A. V. Volyar and T. A. Fadeeva, Opt. Spectrosc. **94**, 235 (2003).
7. J. Leach and M. J. Padgett, New J. Phys. **5**, 154 (2003).
8. I. G. Mariyenko, J. Strohaber, and C. J. G. J. Uiterwaal, Opt. Express **13**, 7599 (2005).
9. G. A. Swartzlander, Jr., Opt. Lett. **31**, 2042 (2006).
10. A. Niv, G. Biener, V. Kleiner, and E. Hasman, Opt. Express **14**, 4208 (2006).
11. Q. Zhan and J. R. Leger, Opt. Commun. **213**, 241 (2002).
12. S. C. Tidwell, G. H. Kim, and W. D. Kimura, Appl. Opt. **32**, 5222 (1993).
13. Y. Yirmiyahu, A. Niv, G. Biener, V. Kleiner, and E. Hasman, Opt. Lett. **31**, 3252 (2006).
14. T. Vallius, J. Turunen, M. Mansuripur, and S. Honkanen, J. Opt. Soc. Am. A **21**, 456 (2004).
15. E. Hasman, G. Biener, A. Niv, and V. Kleiner, in *Progress in Optics* Vol. 47, E. Wolf, ed. (Elsevier, 2005), p. 215.
16. A. Niv, G. Biener, V. Kleiner, and E. Hasman, Opt. Commun. **251**, 306 (2005).
17. N. Bokor, R. Shechter, N. Davidson, A. A. Friesem, and E. Hasman, Appl. Opt. **40**, 2076 (2001).
18. H. Kikuta, Y. Ohira, and K. Iwata, Appl. Opt. **36**, 1566 (1997).
19. M. V. Berry, J. Opt. A, Pure Appl. Opt. **6**, 259 (2004).